

Optical constants of thermally evaporated amorphous GeSe₃ thin films

J. REYES, E. MÁRQUEZ, J.B. RAMÍREZ-MALO, C. CORRALES,
J. FERNÁNDEZ-PEÑA, P. VILLARES, R. JIMÉNEZ-GARAY

*Departamento de Estructura y Propiedades de los Materiales, Facultad de Ciencias,
Universidad de Cádiz, Ap. 40, 11510 Puerto Real (Cádiz), Spain*

The optical transmission spectra of amorphous Ge–Se films of chemical composition GeSe₃, prepared by thermal evaporation, are measured over the 300 nm to 2500 nm spectral region. A simple, straightforward procedure suggested by Swanepoel, which is based on the use of interference fringes, has been applied in order to derive the real and imaginary parts of the complex refractive index, and also the film thickness. Furthermore, thickness measurements made by a surface-profiling stylus are also carried out to cross-check the results obtained by the present optical method, employing only $T(\lambda)$. The dispersion of n is discussed in terms of the single-oscillator Wemple and DiDomenico model, and the optical band gap E_g^{opt} has been determined from the absorption coefficient values, using the Tauc procedure.

1. Introduction

The excellent transmittance of chalcogenide glassy semiconductors [1], reaching up to the far-infrared spectral region, and the wide range of photo-induced effects that they exhibit (such as photocrystallization, photopolymerization, photodecomposition, photovaporization and photodissolution of certain metals), generally accompanied by changes in the optical constants and, particularly, shifts in the absorption edge (i.e. photodarkening or photobleaching), allow their use as absorption filters and other optical elements [2, 3]. Of these effects, metal-photodissolution (particularly, Ag-photodissolution) is probably the most useful one as far as technological applications are concerned, because it produces the largest change in the optical properties of chalcogenide glasses [4]. Therefore, a knowledge of the optical constants of chalcogenide amorphous semiconductors is, indeed, necessary for exploiting their very interesting technological potentials.

The present paper is mainly concerned with the optical characterization of as-deposited a-GeSe₃ thin films prepared by thermal evaporation, using a very accurate data-processing method, based only on their optical transmission spectra [5, 6].

2. Experimental details

The bulk glasses were prepared by direct synthesis from the corresponding elements in evacuated quartz ampoules at about 950 °C for 24 h. After the synthesis the ampoules were air-quenched. Thin-film samples were deposited by vacuum evaporation of powdered glassy material onto clean glass substrates (BDH microscope slides). The thermal evaporation process

was carried out in a coating system (Edwards, model E306A) at a pressure of $\approx 10^{-4}$ Pa from a suitable quartz crucible. The substrates were conveniently rotated at a speed of approximately 50 r.p.m., during the deposition process, by means of a very efficient rotary workholder, which makes it possible to obtain deposited thin films of remarkably uniform thickness [7]. The average deposition rate was ≈ 0.6 nm s⁻¹, and was continuously measured by a quartz crystal monitor (Edwards, model FTM-5). Such a very low deposition rate produces a film composition which is very close to that of the bulk starting material [8] (EDAX-analysis has indicated that the film stoichiometry is correct to ± 1 at %). On the other hand, the lack of crystallinity in the thin films was verified by X-ray diffraction analysis. The thickness of the as-deposited a-GeSe₃ films studied ranged mostly between around 800 nm and 1000 nm, although some thicker films were also prepared.

The optical transmission spectra at normal incidence were obtained by a double-beam UV-VIS-NIR spectrophotometer (Perkin-Elmer, model Lambda-19), and the wavelength range analysed was from 300 nm up to 2500 nm. Finally, a surface-profiling stylus (Sloan, model Dektak IIA) was used to cross-check the film thickness (the difference between the optically determined thickness and the mechanically determined thickness was found to be $\approx 1\%$). All the optical measurements reported in this paper were made at room temperature.

3. Results and discussion

The optical system under consideration corresponds to amorphous, homogeneous and uniform thin films of chemical composition GeSe₃, deposited onto thick,

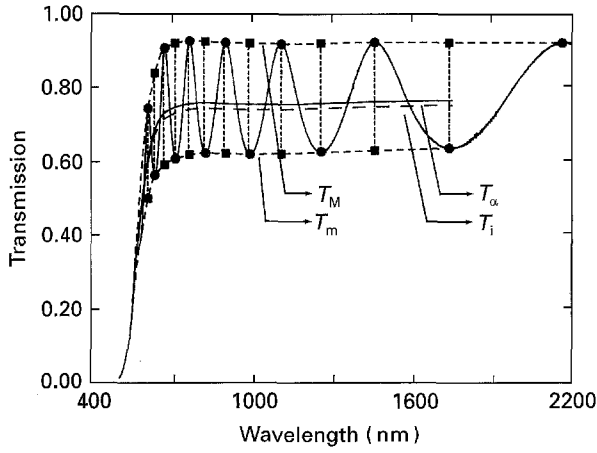


Figure 1 Experimental optical transmission spectrum corresponding to an a-GeSe₃ thin film. Curves T_M and T_m are the maximum and minimum envelopes, respectively. T_i is the curve passing through the inflection points of the interference fringes and T_α is the so-called interference-free transmission curve. (●) Experimental values, (■) calculated values.

finite, transparent substrates. The films have thickness d and complex refractive index $n_c = n - ik$, where n is the refractive index and k the extinction coefficient, which can be expressed in terms of the absorption coefficient α by the equation $k = \alpha\lambda/4\pi$. The thickness of the substrates is several orders of magnitude larger than d , and their refractive index is symbolized by s . Interference effects give rise to oscillating curves like that in Fig. 1. Such interference fringes will be used to determine the optical constants of the thin films under study.

Optical transmission $T(\lambda, s, n, d, k)$ is a very complex function which can be simplified by neglecting the extinction coefficient k , an approximation that is certainly valid over most of the spectrum (Fig. 1 shows that a-GeSe₃ thin films are reasonably transparent over a wide range of the spectrum), so that, with $k = 0$, the expression for T then becomes

$$T(\lambda, s, n, d, k) = \frac{Ax}{B - Cx \cos\phi + Dx^2} \quad (1)$$

where $A = 16n^2s$, $B = (n + 1)^3(n + s)^2$, $C = 2(n^2 - 1) \times (n^2 - s^2)$, $D = (n - 1)^3(n - s^2)$, $\phi = 4\pi nd/\lambda$ and x , the absorbance, is given by the formula $x(\lambda) = \exp(-\alpha d)$. Moreover, the values of the transmission at the

extrema of the interference fringes can be obtained from Equation 1 by setting the interference conditions $\cos\phi = 1$ and $\cos\phi = -1$ for maxima and minima, respectively. The transmission values at the extrema of the interference fringes can then be written as follows:

$$T_M = \frac{Ax}{B - Cx + Dx^2} \quad (2)$$

$$T_m = \frac{Ax}{Bx + Cx + Dx^2} \quad (3)$$

where T_M and T_m are the transmission maximum and the corresponding minimum, respectively (Fig. 1).

In addition, according to Swanepoel's method, which is based on the idea of Manifacier *et al.* [9] of creating the envelopes of interference maxima and minima, a first, approximate value of the refractive index of the film, n_1 , in the spectral region of medium and weak absorption, can be calculated by the following expression:

$$n_1 = [N_1 + (N_1^2 - s^2)^{1/2}]^{1/2} \quad (4)$$

where

$$N_1 = 2s \frac{T_M - T_m}{T_M T_m} + \frac{s^2 + 1}{2}$$

Furthermore, the refractive index of the substrate at each λ was derived by independently measuring the transmittance of the substrate alone, T_s , and using the following equation:

$$s = \frac{1}{T_s} + \left(\frac{1}{T_{s2}} - 1 \right)^{1/2} \quad (5)$$

The values of the refractive index n_1 , as calculated from Equation 4, are listed in Table I. The accuracy of this initial determination of the refractive index is improved after calculating d , taking into account the basic equation for interference fringes:

$$2nd = m\lambda \quad (6)$$

where the order number m is an integer for maxima and half integer for minima. The first, approximate value of the layer thickness is given by the following expression:

$$d_1 = \frac{\lambda_1 \lambda_2}{2(n_{e2} \lambda_1 - n_{e1} \lambda_2)} \quad (7)$$

TABLE I Values of λ , s , T_M and T_m for the a-GeSe₃ transmission spectrum of Fig. 1; calculation of n and d

λ (nm)	s	T_M	T_m	n_1	d_1 (nm)	m_0	m	d_2 (nm)	n_2
1753	1.530	0.921	0.637	2.430	—	2.65	2.5	902	2.419
1465	1.543	0.920	0.630	2.466	—	3.22	3.0	891	2.426
1261	1.550	0.918	0.625	2.486	855	3.77	3.5	888	2.436
1110	1.562	0.917	0.620	2.512	862	4.33	4.0	884	2.451
993	1.549	0.918	0.619	2.508	903	4.83	4.5	891	2.467
901	1.549	0.920	0.620	2.505	967	5.32	5.0	899	2.487
826	1.528	0.923	0.621	2.484	1037	5.75	5.5	914	2.508
765	1.526	0.924	0.615	2.504	1015	6.26	6.0	917	2.534
715	1.516	0.918	0.604	2.524	957	6.75	6.5	921	2.566
672	1.513	0.905	0.588	2.557	940	7.27	7.0	920	2.597
637	1.512	0.842	0.563	2.547	1066	7.64	7.5	938	2.637

$\bar{d}_1 = 956$ nm, $\sigma_1 = 75$ nm (7.8%); $\bar{d}_2 = 906$ nm, $\sigma_2 = 17$ nm (1.9%).

where n_{e1} and n_{e2} are the refractive indices at two adjacent maxima (or minima) at λ_1 and λ_2 . The average value of d_1, \bar{d}_1 , can now be used, along with n_1 , to calculate the 'order number' m_0 for the different extrema, using Equation 6. The accuracy of d can now be significantly increased by taking the corresponding exact integer or half integer values of m associated with each interference extreme, and deriving a new thickness, d_2 , from Equation 6, again using the values of n_1 . With the very accurate value of d , Equation 6 can now be solved for n at each λ , and thus the final values of the refractive index, n_2 , are obtained, and listed in Table I.

Furthermore, a simple, complementary graphical method for deriving the values of m and d , based on the basic equation for interference fringes, was also used [5, 6]. Equation 6 can be rewritten as:

$$\frac{l}{2} = 2d \frac{n}{\lambda} - m_1 \quad (8)$$

where $l = 0, 1, 2, \dots$, and m_1 corresponds to the order number of the first interference extreme of the transmission spectrum. Therefore, plotting $l/2$ against n/λ yields a straight line with gradient $2d$ and intercept on the vertical axis of $-m_1$. Figure 2 shows this plot, which gives the values $d = 955.5$ nm and $m_1 = 2.75$, in excellent agreement with those shown in Table I.

Now, the values of n_2 are fitted to the Wemple–DiDomenico dispersion relationship [10, 11]:

$$n^2(E) = 1 + \frac{E_0 E_d}{E_0^2 - E^2} \quad (9)$$

where E_0 is the single-oscillator energy and E_d the dispersion energy. By plotting $(n^2 - 1)^{-1}$ against E^2 and fitting a straight line as shown in Fig. 3, E_0 and E_d are determined directly from the gradient,

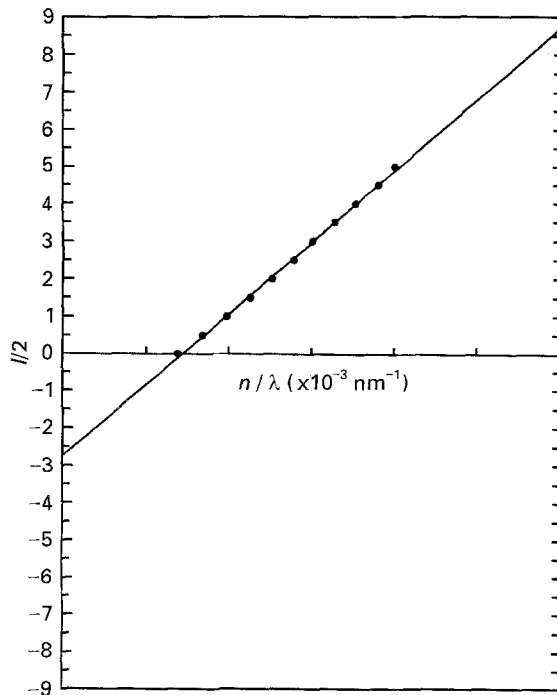


Figure 2 Plot of $l/2$ versus n/λ to determine the order number and film thickness; $m_1 = 2.75$, $2d = 1911$ nm.

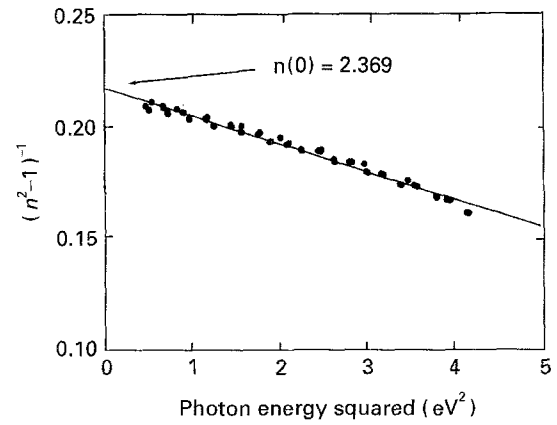


Figure 3 Plot of refractive-index factor $(n^2 - 1)^{-1}$ versus E^2 ($n(0)$ -value is the refractive index extrapolated at $E = 0$). $E_0 = 4.21$ eV, $E_d = 19.43$ eV.

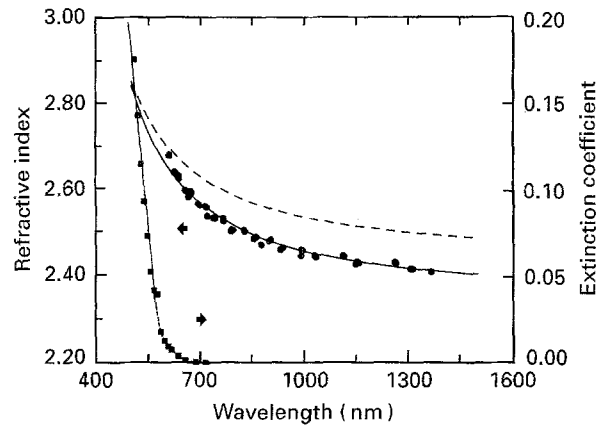


Figure 4 Refractive indices of thermally evaporated a-GeSe₃ thin films against wavelength, and the fit to the Wemple–DiDomenico relationship. Dashed line corresponds to the Wemple–DiDomenico fit for a-GeSe₂ films. Also shown is extinction coefficient k against wavelength. (—) GeSe₃, (---) GeSe₂ [13].

$(E_0 E_d)^{-1}$, and the intercept, E_0/E_d , on the vertical axis [12]. Moreover, Fig. 4 shows the values of the refractive index for five of the GeSe₃ glass films studied, together with the curve corresponding to their least-squares fit to the Wemple–DiDomenico dispersion relationship ($E_0 = 4.21$ eV and $E_d = 19.43$ eV), as well as the dispersion curve of a-GeSe₂ films (from the values $E_0 = 4.60$ eV and $E_d = 23.2$ eV obtained by Theye *et al.* [13]). Additionally, Wemple and DiDomenico have proved that the dispersion parameter E_d obeys the simple empirical relationship, $E_d = \beta N_c Z_a N_e$, where β is a constant, N_c the number of nearest neighbour cations to the anion, Z_a the formal chemical valency of the anion and N_e the effective number of valence electrons per anion [11]. Therefore, in order to account for the compositional trend of E_d , it is suggested that the observed increase in E_d with increasing Ge-content is primarily a coordination number effect [14].

Since the values of the refractive index are already known over the studied spectral region from the above-mentioned optical dispersion relationship, the absorbance $x(\lambda)$ is next calculated in four different ways [5, 12], which are respectively based on the maximum envelope, T_m , the minimum envelope, T_m , the T_x -curve, and finally, on the T_i -curve (T_x is the

interference-free transmission curve, calculated by the expression $T_\alpha = (T_M T_m)^{1/2}$, whereas T_i represents a curve passing through the inflection points of the interference fringes, and it is obtained from the expression $T_i = 2T_M T_m / (T_M + T_m)$. In the region of strong absorption, the interference fringes disappear, and for very large values of α the four curves T_M , T_m , T_α and T_i , converge to a single curve. According to the T_M -based procedure, the absorbance is calculated from the equation

$$x(\lambda) = \frac{E_M - [E_M^2 - (n^2 - 1)^3(n^2 - s^4)]^{1/2}}{(n - 1)^3(n - s^2)} \quad (10)$$

where

$$E_M = \frac{8n^2 s}{T_M} + (n^2 - 1)(n^2 - s^2)$$

The T_m -based procedure is more sensitive to experimental inaccuracies (at energy values under approximately 2.2 eV, its results diverge clearly from those obtained through the other methods). The absorbance expression, according to this method, is given by

$$x(\lambda) = \frac{E_m - [E_m^2 - (n^2 - 1)^3(n^2 - s^4)]^{1/2}}{(n - 1)^3(n - s^2)} \quad (11)$$

where

$$E_m = \frac{8n^2 s}{T_m} - (n^2 - 1)(n^2 - s^2)$$

According to the T_α - and T_i -based procedures, the absorbance is given by the following equations:

$$x(\lambda) = \frac{\{F - [F^2 - (n^2 - 1)^6(n^2 - s^4)^2]^{1/2}\}^{1/2}}{(n - 1)^3(n - s^2)} \quad (12)$$

where

$$F = \frac{128n^4 s^2}{T_\alpha^2} + n^2(n^2 - 1)^2(s^2 - 1)^2 + (n^2 - 1)^2(n^2 - s^2)^2$$

and

$$x(\lambda) = \frac{G - [G^2 - (n^2 - 1)^3(n^2 - s^4)]^{1/2}}{(n - 1)^3(n - s^2)} \quad (13)$$

where

$$G = \frac{8n^2 s}{T_i}$$

Once the absorbance $x(\lambda)$ is known, the relationship $x = \exp(-\alpha d)$ can be solved for α , since $\alpha = -(1/d) \times \ln x$, and thus, the values of the absorption coefficient are finally derived (Fig. 5).

On the other hand, in the Urbach region ($1 \text{ cm}^{-1} < \alpha < \approx 10^4 \text{ cm}^{-1}$) it can be seen that the α -values are smoothly connected, except those that have been calculated from the T_m -curve. In this spectral region, the absorption coefficient depends exponentially upon photon energy, according to the relationship [12, 14]:

$$\alpha(E) = \alpha_0 \exp\left(\frac{E}{K_1}\right) \quad (14)$$

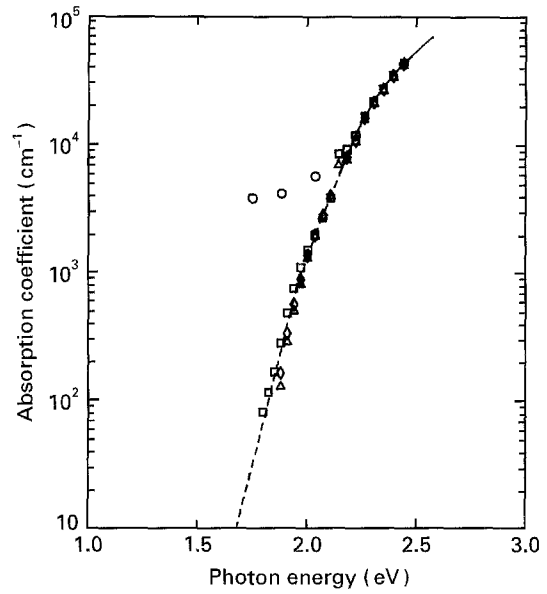


Figure 5 Optical absorption coefficient in the a-GeSe₃ thin film as a function of photon energy. (—) Strong absorption region, (---) Urbach region. (□) T_M , (○) T_m , (△) T_α , (◇) T_i .

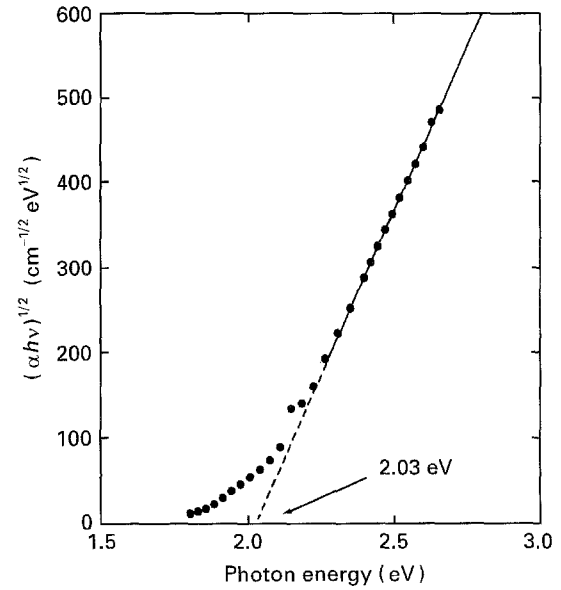


Figure 6 Dependence of $(\alpha h\nu)^{1/2}$ on photon energy $h\nu$ in an a-GeSe₃ thin film from which the optical band gap, E_g^{opt} , is derived (Tauc's extrapolation).

where K_1 is a slope parameter. If the values of α are fitted to this particular relationship, it is found that $K_1 \approx 0.08 \text{ eV}$.

Furthermore, the optical band gap will be obtained from the calculated values of α in the strong-absorption region ($\alpha > \approx 10^4 \text{ cm}^{-1}$). To that end, it should be pointed out that the absorption coefficient, in that spectral region, is given according to Tauc [2, 12] by the following equation:

$$\alpha(E) = \frac{K_2(E - E_g^{\text{opt}})^2}{E} \quad (15)$$

where E , E_g^{opt} and K_2 denote the photon energy, optical band gap and an energy-independent constant, respectively. The optical gap, E_g^{opt} , is formally defined as the intercept of the plot of $(\alpha E)^{1/2}$ against E , as shown in Fig. 6. For the glass composition under

study, GeSe₃, the value of E_g^{opt} is found to be 2.03 eV. On the other hand, according to the α -values derived by Theye *et al.* [13] for the glass composition GeSe₂, the value of E_g^{opt} was found to be 1.99 eV (a lower atomic percentage of Ge in the Ge–Se glassy system yields a higher value for the optical gap). Moreover, the average value of the constant K_2 has been found to be $6.5 \times 10^5 \text{ cm}^{-1} \text{ eV}^{-1}$.

Finally, in order to complete the calculation of the optical constants, the extinction coefficient is determined from the values of α and λ , using the above-mentioned formula $k = \alpha\lambda/4\pi$. Figure 4 also illustrates the dependence of k upon wavelength.

4. Concluding remarks

The optical characterization of amorphous semiconducting thin films prepared by thermal evaporation, using only the optical transmission spectrum at normal incidence, should take into consideration the possible lack of film thickness uniformity, since this feature of the film gives rise to a clear shrinking of the interference fringes of the transmission spectrum [12]. However, in the present work, the very good agreement between the optically- and mechanically-determined thicknesses of the studied a-GeSe₃ thin films, and the excellent results obtained from our systematic study of the optical properties, are a clear consequence of the remarkably uniform thickness of the thin films under study, attained by using the very efficient rotary workholder.

In addition, it should be pointed out that several as-deposited a-GeSe₃ thin films were illuminated by a Hg arc lamp (through an IR-cut filter) and the effect of illumination was the blue-shift of their optical transmission spectra, that is to say, a photo-bleaching process has taken place in the glassy sample [3].

Similarly, after annealing (at 175 °C for 24 h), the as-deposited a-GeSe₃ films showed a thermal-bleaching process. A detailed report on these particular experiments currently underway will be published elsewhere.

References

1. J. A. SAVAGE, "Infrared Optical Materials and their Anti-reflection Coatings" (Hilger, London, 1985).
2. J. TAUC, "Amorphous and Liquid Semiconductors" (Plenum Press, New York, 1974).
3. A. E. OWEN, A. P. FIRTH and P. J. S. EWEN, *Phil. Mag.* **B52** (1985) 347.
4. E. MÁRQUEZ, J. B. RAMÍREZ-MALO, J. FERNÁNDEZ-PEÑA, R. JIMÉNEZ-GARAY, P. J. S. EWEN and A. E. OWEN, *Optical Mater.* **2** (1993) 143.
5. R. SWANEPOEL, *J. Phys. E: Sci. Instrum.* **16** (1983) 1214.
6. E. MÁRQUEZ, J. B. RAMÍREZ-MALO, P. VILLARES, R. JIMÉNEZ-GARAY, P. J. S. EWEN and A. E. OWEN, *J. Phys. D: Appl. Phys.* **25** (1992) 535.
7. K. H. BEHRNDT, in "Physics of Thin Films", edited by G. Hass and R. E. Thun (Academic Press, New York, 1964) p. 46.
8. K. WHITE, B. KUMAR and A. K. RAI, *Thin Solid Films* **161** (1988) 139.
9. J. C. MANIFACIER, J. GASIOT and J. P. FILLARD, *J. Phys. E: Sci. Instrum.* **9** (1976) 1002.
10. S. H. WEMPLE and W. DIDOMENICO, *Phys. Rev.* **B3** (1971) 1338.
11. S. H. WEMPLE, *ibid.* **B7** (1973) 3767.
12. J. B. RAMÍREZ-MALO, E. MÁRQUEZ, P. VILLARES and R. JIMÉNEZ-GARAY, *Mat. Lett.* **17** (1993) 327.
13. M. L. THEYE, M. F. KOTKATA, K. M. KANDIL, A. GHEORGHIU, C. SENEMAUD, J. DIXMIER and F. PRADAL, *J. Non-Cryst. Solids* **137&138** (1991) 963.
14. J. B. RAMÍREZ-MALO, E. MÁRQUEZ, P. VILLARES and R. JIMÉNEZ-GARAY, *Phys. Stat. Sol. (a)* **133** (1992) 499.

Received 20 May 1994

and accepted 21 February 1995